

# Invariant Curves for Area-Preserving Twist Maps far from Integrable

Alessandra Celletti<sup>1</sup> and Luigi Chierchia<sup>2</sup>

Received October 1, 1990; final May 20, 1991

---

One-parameter families of area-preserving twist maps of the form  $F_\varepsilon(x, y) = (x + y + \varepsilon f(x), y + \varepsilon f(x))$  are considered. Various invariant curves, for the maps corresponding to  $f(x) = \sin x$  and  $f(x) = \sin x + (1/50) \sin(5x)$ , are rigorously constructed for large values of the nonlinearity parameter  $\varepsilon$ . For larger values of  $\varepsilon$ , close to critical, some numerical experiments are briefly discussed.

---

**KEY WORDS:** Conservative dynamical systems; twist maps; invariant curves; KAM theory; effective stability estimates.

## 1. INTRODUCTION

Consider one-parameter families of area-preserving twist maps of the form

$$F_\varepsilon: \begin{cases} y' = y + \varepsilon f(x) \\ x' = x + y' \pmod{2\pi} \end{cases} \quad (1)$$

where  $y \in \mathbf{R}$ ,  $x \in \mathbf{T} \equiv \mathbf{R}/2\pi\mathbf{Z}$ ,  $\varepsilon$  is a real parameter, and  $f(x)$  is a periodic real-analytic function with zero average.

For  $\varepsilon = 0$ ,  $F_0$  is *integrable*: all trajectories lie on circles,  $\{y = \text{const}\} \equiv \mathcal{C}_0(y) \subset \mathbf{R} \times \mathbf{T}$ , and the dynamics is simply a rotation by  $y$ . When  $\varepsilon \neq 0$  but small it can be shown by KAM theory<sup>(1,18,25)</sup> (see ref. 11 for an elementary exposition, and ref. 4 for a review) that for most (in measure-theoretic sense) numbers  $\omega$  there still exists a unique analytic invariant curve  $\mathcal{C}_\varepsilon(\omega)$  (homotopically nontrivial) on which the dynamics is described, up to an analytic change of variables, by a rotation by  $\omega$  as in

---

<sup>1</sup> Dipartimento di Matematica Pura e Applicata, Università dell'Aquila, L'Aquila, Italy.

<sup>2</sup> Dipartimento di Matematica, II Università di Roma "Tor Vergata", 00133 Rome, Italy.

the integrable case. Here, we shall call curves  $\mathcal{C}_\varepsilon(\omega)$  ( $\varepsilon \neq 0$ ) satisfying the just mentioned properties, KAM curves.

A byproduct of KAM theory is that the set of parameter values  $\varepsilon$  for which  $\mathcal{C}_\varepsilon(\omega)$  exists and is analytic is open. Therefore, for each of the above  $\omega$ , we can define a value  $\varepsilon_a(\omega)$  corresponding to the “last KAM curve”: the open interval  $(0, \varepsilon_a)$  is the maximal interval of the form  $(0, a)$  such that for every  $0 < \varepsilon < a$  there exists a KAM curve  $\mathcal{C}_\varepsilon(\omega)$ .

On the other hand, it can be shown<sup>(24)</sup> that if  $\varepsilon$  is large enough,  $F_\varepsilon$  admits no continuous invariant, homotopically nontrivial, circles at all. Another critical parameter value can therefore be defined:

$$\varepsilon_b(\omega) \equiv \sup \{ \varepsilon_0 \geq 0 \text{ s.t. } F_\varepsilon \text{ admits a continuous invariant circle with rotation number } \omega, \text{ for all } \varepsilon \in [0, \varepsilon_0] \}$$

where “circle” is short for “homotopically nontrivial embedding of  $\mathbf{T}$  into  $\mathbf{R} \times \mathbf{T}$ ” and by “rotation number” we mean the Poincaré rotation number of the circle map obtained by restricting  $F_\varepsilon$  to the invariant circle (for general information see, e.g., ref. 14).

Natural questions such as the relation between  $\varepsilon_a$  and  $\varepsilon_b$ , the dependence of the curve on (the number-theoretic properties of)  $\omega$ , and the mechanism beyond the disappearance of the invariant curves as  $\varepsilon$  is increased are still mathematically unexplained. Partial answers can, however, be extracted from refs. 6, 10, 14, 15, 22, and 23. The results of refs. 22 and 6 exploit *computer-assisted* techniques, i.e., techniques involving long (but straightforward) calculations, which are performed with the aid of computers; the so-called *interval arithmetic* is used to control rigorously the numerical errors introduced by the machine (see refs. 19 and 9 and Appendix C below).

The results of ref. 6 together with the upper bounds on  $\varepsilon_b$  of ref. 22 suggest that, at least in the case of the so-called standard map (*SM*) [i.e., (1) with  $f(x) = \sin(x)$ ]

$$\sup_{\omega} \varepsilon_b(\omega) \equiv \varepsilon_a(\omega_*) \tag{2}$$

for a particular rotation number  $\omega_*$ , which, in the case of the (*SM*), seems to be  $2\pi$  times the golden mean  $(\sqrt{5} - 1)/2$ .

Here, we consider the (*SM*) and the map (1) with  $f(x) = \sin(x) + (1/50) \sin(5x)$  [dubbed (*SM*)'] and, extending and refining the techniques of ref. 6, we construct KAM curves for the following rotation numbers  $\omega_k \in (0, 2\pi)$ :

$$\frac{\omega_1}{2\pi} \equiv \frac{\sqrt{5} - 1}{2}, \quad \frac{\omega_2}{2\pi} \equiv \frac{\sqrt{5} + 5}{10}, \quad \frac{\omega_3}{2\pi} \equiv \frac{\sqrt{2}}{2} \tag{3}$$

for “large” values of the nonlinearity parameter  $\varepsilon$ , “large” meaning  $\varepsilon = O(\varepsilon_b)$  (see below for the exact numbers and for the experimental calculation of  $\varepsilon_b$ ). These curves and some of their properties are also investigated numerically.

To be more precise, denote by  $\mathcal{C}_\varepsilon(\omega_k)$  the invariant curve with rotation number  $\omega_k$  for the standard map and by  $\mathcal{C}'_\varepsilon(\omega_k)$  the invariant curve for the map  $(SM)'$ . In Section 2, implementing the KAM technique presented in ref. 6, we construct  $\mathcal{C}_\varepsilon(\omega_k)$  and  $\mathcal{C}'_\varepsilon(\omega_k)$  for  $\varepsilon \in \mathbb{C}$  with  $|\varepsilon| \leq \rho_k$ ,  $|\varepsilon| \leq \rho'_k$ , respectively, proving the existence of  $\mathcal{C}_\varepsilon(\omega_1)$  for  $|\varepsilon| \leq 0.838$ , of  $\mathcal{C}_\varepsilon(\omega_2)$  for  $|\varepsilon| \leq 0.77$ , of  $\mathcal{C}_\varepsilon(\omega_3)$  for  $|\varepsilon| \leq 0.76$ , of  $\mathcal{C}'_\varepsilon(\omega_1)$  for  $|\varepsilon| \leq 0.4$ , and of  $\mathcal{C}'_\varepsilon(\omega_2)$  for  $|\varepsilon| \leq 0.39$ . All these results are new; the only curve which has been investigated along these lines is  $\mathcal{C}_\varepsilon(\omega_1)$ . In ref. 6 the existence of  $\mathcal{C}_\varepsilon(\omega_1)$  was proved for  $|\varepsilon| \leq 0.65$ . The main reason for the present improvement lies in a change related to the “choice” of the *initial approximation* used as starting point for the *KAM algorithm*. More precisely, while in ref. 6 we used interval arithmetic also in the first stage of constructing the initial guess for the Newton method, here we choose a *numerically* constructed initial approximation and apply interval arithmetic only at later stages when the accuracy of the initial guess is rigorously controlled. This change of strategy has the advantage of avoiding the use of interval arithmetic *directly* on small divisors, reducing in a conspicuous way the sensitivity of the computations (see Section 2.3).

In Section 3, following Greene,<sup>(13)</sup> we give a numerical evaluation of  $\varepsilon_a$  (which we shall compare with a numerical extrapolation of our KAM algorithm).

The agreement between our rigorous lower bounds and the numerical evaluation of  $\varepsilon_b$  is within 86%–54%. Analogous results for the golden mean invariant curve for the standard map have been announced in ref. 8, where it is claimed that such a curve exists for  $\varepsilon = 0.91$ . The strategy in ref. 8, which seems to be not completely unrelated to ours, allows one to handle higher nonlinearities; however, their method does not give any global information in parameter space. For example, they do not establish the existence of the golden mean curve for  $\varepsilon \in [0, 0.91]$ .

The curves we construct are *analytic in the parameter*  $\varepsilon$  in complex disks around  $\varepsilon = 0$ ; therefore the efficiency of our method is clearly related to the distribution of (complex) *singularities in the parameter*  $\varepsilon$ . This is briefly discussed in Section 3.2 (see also ref. 3). Finally, in Section 3.3 we reproduce a few graphs indicating the self-similar nature of the invariant curves as  $\varepsilon \simeq \varepsilon_a$  (the self-similarity of critical invariant curves is one of the main themes in the *renormalization approach*<sup>(10,21)</sup>).

## 2. CONSTRUCTION OF INVARIANT CURVES

Consider maps as in (1) and fix  $\omega \in (0, 2\pi)$  so that  $\omega/2\pi$  satisfies the diophantine condition

$$\left| \frac{\omega}{2\pi} q - p \right|^{-1} \leq C |q|^\tau, \quad \forall p, q \in \mathbf{Z}, \quad q \neq 0 \quad (4)$$

for some positive constants  $C$  and  $\tau$ . For example, for  $\omega = \omega_i$  as in (3) one has  $\tau = 1$  and  $C_1 \equiv (3 + \sqrt{5})/2$ ,  $C_2 \equiv (5 + \sqrt{5})/2$ , and  $C_3 \equiv 2 + \sqrt{2}$  (see Appendix A).

A KAM curve with rotation number  $\omega$  is defined by the parametric equations

$$\begin{cases} x = x(\theta; \varepsilon) \equiv \theta + u(\theta; \varepsilon), & 1 + u_\theta \neq 0 \\ y = y(\theta; \varepsilon) \end{cases} \quad (5)$$

where  $u(\cdot, \varepsilon)$ ,  $y(\cdot, \varepsilon)$  are real-analytic  $2\pi$ -periodic functions of  $\theta \in \mathbf{T}$  and are such that

$$F_\varepsilon(x(\theta; \varepsilon), y(\theta; \varepsilon)) = (x(\theta + \omega; \varepsilon), y(\theta + \omega; \varepsilon)), \quad \forall \theta \in \mathbf{T} \quad (6)$$

Since  $y' = x' - x$  [see (1)],  $y$  is related to  $u$  in (5) simply by

$$y(\theta; \varepsilon) \equiv \omega + u(\theta; \varepsilon) - u(\theta - \omega; \varepsilon), \quad \forall \theta \in \mathbf{T} \quad (7)$$

so that, eliminating the function  $y$  in (6), one obtains the following nonlinear, finite-difference equation for  $u$ :

$$D^2 u - \varepsilon f(\theta + u) = 0 \quad (1 + u_\theta \neq 0) \quad (8)$$

where  $D$  denotes the operator

$$(Du)(\theta) = u\left(\theta + \frac{\omega}{2}\right) - u\left(\theta - \frac{\omega}{2}\right)$$

(here and below we drop the explicit dependence upon the parameter  $\varepsilon$  when this does not lead to confusion). Conversely, if  $u$  is a real-analytic solution of (8), then *defining*  $x(\theta)$  as in the first line of (5) and  $y(\theta)$  as in (7), one can easily check that  $(x(\theta), y(\theta))$  is a KAM curve satisfying (6). Thus the problem of the existence of KAM curves reduces to finding analytic solutions of (8).

Notice that if  $u(\theta)$  is a solution of (8), then so is  $c + u(\theta + c)$  for any constant  $c$ ; for definiteness we shall impose that  $u$  has vanishing mean value.

### 2.1. KAM Algorithm

As in ref. 6, to solve (8) *efficiently* we shall use a Newton iteration procedure equipped with a set of careful estimates.

Let  $v^{(0)}$  be an initial approximation, i.e., a real-analytic  $2\pi$ -periodic function with vanishing average on  $\mathbb{T}$ , with  $1 + v_\theta^{(0)} \neq 0$  and such that the error  $e^{(0)}$  defined by the equation

$$D^2v^{(0)} - \varepsilon f(\theta + v^{(0)}) = e^{(0)} \tag{9}$$

is *small* (see below for the precise meaning of “small”).

Then a sequence of better and better approximations  $\{v^{(j)}\}$  satisfying

$$D^2v^{(j)} - \varepsilon f(\theta + v^{(j)}) = e^{(j)}, \quad 1 + v_\theta^{(j)} \neq 0 \tag{10}$$

is constructed as follows. Consider the equation for  $w$

$$D[\phi_j^+ \phi_j^- D(\phi_j^{-1}w)] = -\phi_j e^{(j)}, \quad \int w \, d\theta = 0 \tag{11}$$

where  $\phi_j \equiv 1 + v_\theta^{(j)}$  and  $+/-$  denotes translations by  $\omega/2$ :

$$\phi^\pm(\theta) \equiv \phi\left(\theta \pm \frac{\omega}{2}\right)$$

Notice that since

$$\int Dg \equiv \int g^+ - g^- = 0 \tag{12}$$

for any periodic function  $g(\theta)$ , Eq. (11) makes sense only if its right-hand side has mean value 0. That this is the case is a consequence of (10): observing that, since  $\int f = 0$ ,  $f = \partial_\theta \tilde{f}$ , an integration by parts and (12) show

$$\begin{aligned} \int \phi_j e^{(j)} &\equiv \int (1 + v_\theta^{(j)}) [D^2v^{(j)} - \varepsilon f(\theta + v^{(j)})] \, d\theta \\ &\equiv \int [v_\theta^{(j)} D^2v^{(j)} + \varepsilon \partial_\theta \tilde{f}(\theta + v^{(j)})] \, d\theta \\ &\equiv \int v_\theta^{(j)} D^2v^{(j)} \, d\theta \end{aligned}$$

and observing that  $D$  satisfies the rule

$$\int g_1 Dg_2 = - \int g_2 Dg_1 \tag{13}$$

for any two functions  $g_k$  on  $\mathbf{T}$ , one concludes that

$$\int \phi_j e^{(j)} = 0 \tag{14}$$

Now, if  $g$  is an analytic function with zero average, we shall denote by  $D^{-1}g$  the unique analytic solution of  $Dh = g$  with zero average. Explicitly, in terms of the Fourier expansion of  $g$ :

$$\begin{aligned} g &\equiv \sum_{n \in \mathbf{Z}, n \neq 0} \hat{g}_n e^{in\theta} \\ D^{-1}g &= \sum_{n \neq 0} \frac{\hat{g}_n}{2i \sin(n\omega/2)} e^{in\theta} \end{aligned} \tag{15}$$

Notice that the analyticity of  $D^{-1}g$  is a consequence of (4). After these observations it is clear that (11) has a unique (analytic) solution,  $w^{(j)}$ . Let

$$v^{(j+1)} = v^{(j)} + w^{(j)} \tag{16}$$

Then it is not difficult to check that  $e^{(j+1)}$  is actually equal to

$$\begin{aligned} e^{(j+1)} &\equiv e_{\theta}^{(j)} \phi_j^{-1} w^{(j)} - \varepsilon [f(\theta + v^{(j)} + w^{(j)}) - f(\theta + v^{(j)}) \\ &\quad - f_x(\theta + v^{(j)}) w^{(j)}] \end{aligned} \tag{17}$$

so that, as we shall see more precisely in a moment, the size of  $e^{(j+1)}$  is *quadratically* smaller than the size of  $e^{(j)}$ . In fact, differentiating (10) with respect to  $\theta$ , one sees that

$$f_x(\theta + v^{(j)}) = \phi_j^{-1} (D^2 v_{\theta}^{(j)} - e_{\theta}^{(j)})$$

so that from the definitions (16) and (17), from the fact that  $D^2 \phi_j = D^2 v_{\theta}^{(j)}$ , and from (11) it follows that

$$\begin{aligned} D^2 v^{(j+1)} - \varepsilon f(\theta + v^{(j+1)}) &= \phi_j^{-1} (\phi_j e^{(j)} + \phi_j D^2 w_j - w_j D^2 \phi_j) + e^{(j+1)} \\ &= \phi_j^{-1} \left( \phi_j e^{(j)} + D \left[ \phi_j^+ \phi_j^- D \left( \frac{w_j}{\phi_j} \right) \right] \right) + e^{(j+1)} \\ &= e^{(j+1)} \end{aligned}$$

From (11), it follows that, roughly speaking,  $w^{(j)}$  has the same “order of magnitude” as  $e^{(j)}$ , so that, if  $e^{(j)}$  is “small” enough,  $v^{(j+1)}$  in (16) will satisfy  $1 + v_{\theta}^{(j+1)} \neq 0$ .

To control such a construction, one needs to introduce suitable norms on analytic periodic functions. The choice of the norms depends on a finite set of auxiliary positive parameters.

For a function  $g = g(\theta, \varepsilon)$  real-analytic in  $(\theta, \varepsilon)$  for  $\theta \in S_\xi \equiv \{\theta \in \mathbf{C}: |\operatorname{Im}(\theta)| \leq \xi\}$ ,  $\xi > 0$  and for  $\varepsilon \in \mathcal{E}$ , where  $\mathcal{E}$  is the closure of a complex open neighborhood of the origin  $\varepsilon = 0$ , we set

$$\|g\|_\xi \equiv \sup_{S_\xi \times \mathcal{E}} |g(\theta, \varepsilon)|$$

(in the following the domain  $\mathcal{E}$  is fixed once and for all and therefore we do not indicate it explicitly in the norm symbols).

**Remark 1.** In ref. 6 we considered  $\mathcal{E} = \{\varepsilon \in \mathbf{C}: |\varepsilon| \leq \rho\}$ , but, as one can easily check, all estimates in this section hold for more general domains  $\mathcal{E}$ .

Now assume that an initial approximation  $v^{(0)}$ , analytic in  $S_\xi \times \mathcal{E}$ , is given (in the next section we shall discuss the choice of  $v^{(0)}$ ) and that

$$\|\phi_0^{-1}\|_\xi \equiv \|(1 + v_\theta^{(0)})^{-1}\|_\xi < \infty$$

Fix  $N \geq 1$  and let  $\delta_0, \dots, \delta_{N-1}$  be positive numbers such that

$$\xi_N \equiv \xi - (\delta_0 + \dots + \delta_{N-1}) > 0$$

For any  $j \geq 0$  let  $M^{(j)}, \tilde{M}^{(j)}, V^{(j)}, V_1^{(j)}, E^{(j)}$  be upper bounds on, respectively,  $\phi_j \equiv 1 + v_\theta^{(j)}, \phi_j^{-1}, v^{(j)}, v_\theta^{(j)}, e^{(j)}$ .

We can now describe the *KAM algorithm*, i.e., a set of recursive relations connecting  $M^{(j)}, \tilde{M}^{(j)}, V^{(j)}, V_1^{(j)}, E^{(j)}$  and  $M^{(j+1)}, \tilde{M}^{(j+1)}, V^{(j+1)}, V_1^{(j+1)}, E^{(j+1)}$  for  $0 \leq j \leq N-1$  and a condition on  $M^{(N)}, \tilde{M}^{(N)}, V^{(N)}, V_1^{(N)}, E^{(N)}$ , which, if satisfied, implies the existence of a KAM curve  $u(\theta; \varepsilon)$  analytic in  $S_{\xi_N/2} \times \mathcal{E}$ .

For  $l = 0, 1$  and  $\delta > 0$  let  $s_l(\delta)$  be an upper bound on the convergent series

$$\left[ \sum_{n=1}^{\infty} \left( \frac{n^l}{\sin(n\omega/2)} \right)^2 e^{-\delta n} \right]^{1/2} \leq s_l(\delta)$$

[an explicit evaluation of  $s_l(\delta)$  is provided in Appendix B] and, for  $0 \leq j \leq N-1$ , let

$$a_j \equiv [M^{(j)} \tilde{M}^{(j)} s_0(\delta_j)]^2 \left\{ 1 + (M^{(j)} \tilde{M}^{(j)})^2 \frac{s_0(2\xi_j)}{s_0(\delta_j)} \right\}$$

where  $\xi_0 = \xi$  and (for  $j \geq 1$ )  $\xi_j = \xi_{j-1} - \delta_{j-1}$ ,

$$W^{(j)} \equiv E^{(j)} a_j$$

and

$$W_1^{(j)} \equiv E^{(j)} a_j \left( \frac{V_1^{(j)}}{M^{(j)}} \delta_j^{-1} + \frac{s_1(\delta_j)}{s_0(\delta_j)} \right)$$

Then one can take (for  $0 \leq j \leq N-1$ )

$$\begin{aligned} M^{(j+1)} &\equiv M^{(0)} + \sum_{i=0}^j W_1^{(i)} \\ \tilde{M}^{(j+1)} &\equiv \begin{cases} \tilde{M}^{(j)} \cdot \left( 1 - \tilde{M}^{(j)} \sum_{i=0}^j W_1^{(i)} \right)^{-1} & \text{if } \sum_{i=0}^j W_1^{(i)} < 1 \\ \infty & \text{if } \sum_{i=0}^j W_1^{(i)} \geq 1 \end{cases} \\ V^{(j+1)} &\equiv V^{(0)} + \sum_{i=0}^j W^{(i)} \\ V_1^{(j+1)} &\equiv V_1^{(0)} + \sum_{i=0}^j W_1^{(i)} \end{aligned}$$

and

$$E^{(j+1)} = (E^{(j)})^2 a_j \left( \frac{a_j F_2^{(j+1)}}{2} + \frac{\delta_j^{-1}}{M^{(j)}} \right)$$

where

$$F_2^{(j+1)} \equiv \| \partial_{xx}^2 f \|_{\xi_{j+1} + V^{(j+1)}}$$

Of course this construction makes sense provided  $\tilde{M}^{(j)} < \infty$ ,  $\forall 1 \leq j \leq N$ . This is a smallness requirement on  $E^{(0)}$ .

The fact that, with these definitions,  $M^{(j+1)}$ ,  $\tilde{M}^{(j+1)}$ ,  $V^{(j+1)}$ ,  $V_1^{(j+1)}$ , and  $E^{(j+1)}$  are upper bounds on  $\|\phi_{j+1}\|_{\xi_{j+1}}$ ,  $\|\phi_{j+1}^{-1}\|_{\xi_{j+1}}$ ,  $\|v^{(j+1)}\|_{\xi_{j+1}}$ ,  $\|v_\theta^{(j+1)}\|_{\xi_{j+1}}$ , and  $\|e^{(j+1)}\|_{\xi_{j+1}}$  is a quite straightforward consequence of the definition of  $w^{(j)}$ , of (17), and of the following quantitative elementary lemma which is proved in ref. 6 (Lemmas 2 and 3 and Appendix A of ref. 6):

**Lemma.** Let  $h = h(\theta, \varepsilon)$  be an analytic function on  $S_\xi \times \mathcal{E}$  with  $\int_{\mathcal{T}} h(\theta, \varepsilon) d\theta = 0$ . Then, for any  $0 < \delta \leq \xi$ ,

$$\begin{aligned} \|h_\theta\|_{\xi-\delta} &\leq \|h\|_{\xi} \delta^{-1} \\ \|\partial_\theta^l D^{-1} h\|_{\xi-\delta} &\leq s_l(2\delta) \|h\|_{\xi} \end{aligned}$$



Finally, assuming (without loss of generality) that  $M^{(N)}, \tilde{M}^{(N)}, \xi_N^{-1} \geq 1$ , one can show (see Lemma 5 of ref. 6) that, taking in (4)  $\tau = 1$  for simplicity, if

$$K \equiv 154 \cdot 10^{13} C^5 (M^{(N)})^2 (M^{(N)} \tilde{M}^{(N)})^{21/2} \xi_N^{-8} F_2^{(N)} E^{(N)} \leq 1 \tag{18}$$

then there exists a unique solution  $u$  of (8), real analytic in  $S_{\xi_N/2} \times \mathcal{E}$ , and such that

$$\|u - v^{(N)}\|_{\xi_N/2} \leq K \xi_N / 64, \quad \|u_\theta - v_\theta^{(N)}\| \leq K/2 \tilde{M}^{(N)} \tag{19}$$

Notice that the numbers  $\xi, N, \delta_1, \dots, \delta_N$  are free parameters (with the constraint that  $\xi_N > 0$ ), which may (and have to) be “optimized.” Such an optimization problem is a rather difficult one from an abstract point of view. However, in concrete cases, because of the fast (quadratic) speed of this algorithm, it is not so hard to make “good” choices.

**Remark 2.** The KAM condition (18) is obviously related to the above iteration scheme: it is a condition that ensures the possibility of iterating the scheme infinitely many times ( $N \leq j \uparrow \infty$ ) so that

$$\tilde{M}_j < \infty \quad \forall j, \quad E^{(j)} \xrightarrow{j \rightarrow \infty} 0 \tag{20}$$

[where for  $j \geq N$  one can take  $\xi_j = (\xi_N/2)(1 + 1/2^j)$ ]. The main step in the derivation of the KAM condition consists in showing that if  $E^{(N)}$  is small enough, then

$$E^{(N+j)} \leq (\bar{K} E^{(N)})^{2j} \tag{21}$$

where  $\bar{K}$  is basically the constant appearing in (18).

**Remark 3.** Of course one can take  $N = 0$ , i.e.,  $v^{(N)} \equiv v^{(0)}$  and apply the KAM condition directly to  $v^{(0)}$ . But the KAM condition is, as it stands, necessarily rather stringent and, as already pointed out elsewhere,<sup>(5-7)</sup> the main point of introducing the KAM *algorithm* is to mitigate the smallness requirements by following carefully the first few steps of the iteration scheme.

### 2.2. Epsilon-Expansions

Taking  $v^{(0)} \equiv 0$  (see Remark 3 above) one has  $e^{(0)}(\theta, \varepsilon) \equiv -\varepsilon f(\theta)$  and the KAM condition is certainly fulfilled by choosing  $\mathcal{E} = \{\varepsilon \in \mathbf{C}: |\varepsilon| \leq \rho\}$  with  $\rho > 0$  small enough. Then, the uniformity in  $\mathcal{E}$  of all estimates implies

that the (unique) solution  $u(\theta, \varepsilon)$  is *real-analytic* also in the parameter  $\varepsilon$ . This means that  $u$  can be represented as a *convergent power series* in  $\varepsilon$ :

$$u(\theta, \varepsilon) = \sum_{l=1}^{\infty} u_l(\theta) \varepsilon^l \tag{22}$$

- Remark 4.** (i) Such a series is sometimes called a Lindstedt series.  
 (ii) The normalization condition  $\int_{\mathbf{T}} u \, d\theta = 0$  implies that

$$\int u_l \, d\theta = 0, \quad \forall l \geq 1 \tag{23}$$

(iii) Inserting (22) into Eq. (8), expanding in  $\varepsilon$ , and equating terms of equal power, one sees that  $u_l$  is related to  $u_1, \dots, u_{l-1}$  by a *linear* equation:

$$D^2 u_l = \Phi_l(u_1, \dots, u_{l-1}) \equiv \frac{1}{(l-1)!} \left. \frac{d^{(l-1)}}{d\varepsilon^{(l-1)}} \right|_{\varepsilon=0} f\left(\theta + \sum_{k=1}^{\infty} \varepsilon^k u_k\right) \tag{24}$$

- (iv) Integrating (24) over  $\mathbf{T}$  shows that

$$\int \Phi_l = 0, \quad \forall l$$

which is a *compatibility* condition among the  $u_l$ .

The rest of this section is devoted to finding explicit and *compact* recursive formulas for computing the  $u_l$  from (24) (see also refs. 12, 17, and 27) and in the next section we shall discuss how to construct initial approximations for the KAM algorithm considering suitable truncations of the Lindstedt series. Let

$$f(\theta) \equiv \sum_{n \neq 0} f_n e^{in\theta}$$

and for any  $n \neq 0$  define the complex-analytic function  $a_k^{(n)}(\theta)$  as the coefficients of the  $\varepsilon$ -expansion of  $e^{in(\theta + u(\theta))}$ , i.e.,

$$e^{in(\theta + u(\theta))} = \sum_{k=0}^{\infty} a_k^{(n)}(\theta) \varepsilon^k \tag{25}$$

Differentiating (25) with respect to  $\varepsilon$ , one obtains

$$in \sum_{l=1}^{\infty} l u_l \varepsilon^{l-1} \sum_{k=0}^{\infty} a_k^{(n)} \varepsilon^k = \sum_{k=1}^{\infty} k a_k^{(n)} \varepsilon^{k-1}$$

or, equivalently,

$$in \sum_{k=1}^{\infty} \left( \sum_{l=1}^{\infty} lu_l a_{k-l}^{(n)} \right) \varepsilon^{k-1} = \sum_{k=1}^{\infty} k a_k^{(n)} \varepsilon^{k-1}$$

so that

$$\begin{cases} a_0^{(n)} = e^{in\theta} \\ a_k^{(n)} = \frac{in}{k} \sum_{h=1}^k hu_h a_{k-h}^{(n)}, \quad k \geq 1 \end{cases} \tag{26}$$

Then, from Eq. (8) it follows that

$$u_l = D^{-2} \sum_{n \neq 0} f_n a_{l-1}^{(n)}(\theta) \tag{27}$$

completing the determination of  $u_l$  in terms of  $u_{l-1}, \dots, u_1$  and of the auxiliary functions  $a_k^{(n)}$ ,  $0 \leq k \leq l-1$ . Notice that, because of (iv) of Remark 4, in deriving (27) we do not need to check directly that the series in (27) has vanishing average over  $\mathbf{T}$  (so as to be able to apply the operator  $D^{-2}$ ). Recall that the operator  $D^{-2}$  is diagonal in Fourier space, being just the multiplication of the  $m$ th Fourier coefficient by

$$\left[ -4 \sin^2 \left( \frac{m\omega}{2} \right) \right]^{-1} = \{ 2[\cos(m\omega) - 1] \}^{-1} \tag{28}$$

Observe also that since  $u(\theta, \varepsilon)$  is real-analytic both in  $\varepsilon$  and  $\theta$ , one has  $u_l \equiv \bar{u}_l$  [where, as usual, for an analytic function  $h(z)$ ,  $\bar{h}(z)$  denotes the analytic function  $\overline{h(\bar{z})}$ ]. Then it follows easily by induction on  $k$  that

$$a_k^{(-n)}(\theta) = \bar{a}_k^{(n)}(\theta) \equiv \overline{a_k^{(n)}(\bar{\theta})} \tag{29}$$

so that

$$u_l = D^{-2} \left( \sum_{n \geq 1} f_n a_{l-1}^{(n)} + \bar{f}_n \bar{a}_{l-1}^{(n)} \right) \tag{30}$$

A case of particular interest to us is when  $f$  is an odd trigonometric polynomial

$$f(\theta) = \sum_{j=1}^r b_j \sin(p_j \theta) \tag{31}$$

where  $p_j, r \in \mathbf{Z}_+, 0 \neq b_j \in \mathbf{R}$ . In this case it is not difficult to see that also the  $u_l$  are odd trigonometric polynomials

$$\begin{aligned} u_l(\theta) &= \sum_{j=1}^{r_l} c_j^{(l)} \sin(m_j^{(l)}\theta) \\ &= \frac{1}{2i} \sum_{j=1}^r b_j D^{-2}(a_{l-1}^{(p_j)} - \bar{a}_{l-1}^{(p_j)}) \end{aligned} \tag{32}$$

for suitable numbers  $r_l, m_j^{(l)} \in \mathbf{Z}_+, 0 \neq c_j^{(l)} \in \mathbf{R}$ .

As a side remark we mention here that for (SM) the number of Fourier coefficients  $c_j^{(l)}$  is given by  $l(l+2)/2$  if  $l$  is even and  $(l+1)^2/2$  if  $l$  is odd.

### 2.3. Initial Approximation

As initial approximation  $v^{(0)}$  of the KAM algorithm of Section 2.1 we would like to take the  $l_0$  truncation of the Lindstedt series (22) with  $l_0$  as large as possible. Since we know that the Lindstedt series is convergent, we expect to be able to give accurate lower bounds on

$$\rho_a = \inf_{\theta \in \mathbf{T}} (\overline{\lim} |u_n(\theta)|^{1/n})^{-1} \tag{33}$$

provided we can find an *effective* way of estimating the error term. Notice that  $\rho_a \leq \varepsilon_a$  (defined in the introduction), the strict inequality being related to the form of the  $\varepsilon$ -domain of analyticity. For the standard map with  $\omega_1$  it is believed that  $\rho_a = \varepsilon_a = \varepsilon_b$ .<sup>(3)</sup>

To carry out this strategy, it is natural to turn to computers: one needs to write a (straightforward) program on the basis of formulas (26)–(32), which computes the Taylor–Fourier coefficients of (a polynomial truncation of) the function  $u$  in (22). However, in doing so one introduces *numerical errors*. In fact, the computer will produce *some rational approximations* (depending on the machine, on the way the program is written, etc.) of the true Taylor–Fourier coefficients of  $u$ .

Nevertheless, as initial approximation we shall define

$$v^{(0)} = \sum_{l=1}^{l_0} \tilde{u}_l(\theta) \varepsilon^l \equiv \sum_{l=1}^{l_0} \sum_{n \neq 0} \tilde{u}_n^{(l)} e^{in\theta} \varepsilon^l \tag{34}$$

where the  $\tilde{u}_l$  are the result of a (given) automatic computation based on the formulas (26)–(32). This is the main difference from ref. 6, where we defined  $v^{(0)} = \sum_{l=1}^{l_0} u_l \varepsilon^l$  and then used the so-called interval arithmetic to keep track of the numerical errors. Here, the interval arithmetic is not used at this stage, but will come in estimating the error term associated to (34).

The interval arithmetic consists, in short, in the following. The numbers *representable* on a computer are, basically, numbers with a finite binary expansion and, depending on the machine one is using, it is possible to give upper and lower bounds, in terms of representable numbers, of the result of elementary operations between representable numbers. Therefore, trapping real numbers with intervals whose ends are representable numbers, it is possible to trap the result of an elementary operation in terms of lower and upper bounds on the result of the operation between the ends of the intervals (see ref. 19 and Appendix C for more details).

The main advantage in defining  $v^{(0)}$  as in (34) rather than as the *theoretical*  $l_0$  truncation of (22) is that we do not need to use interval arithmetic at this stage (as we did in ref. 6) and therefore we *do not use interval arithmetic* on the small divisors (28) appearing in (27). Of course, we shall pay for it later when we can no longer use the fact that the  $l_0$  truncation of (22) *solves exactly* Eq. (8) up to order  $l_0$  in  $\varepsilon$ . Instead we will have to rigorously control the job of our machines and check (with interval arithmetic) how far from the theoretical guess is the polynomial (34) evaluated by the computer. Notice, however, that in this “validation stage” small divisors do not appear directly. This fact makes quite a lot of difference.

### 2.4. Bound on the Error Term

In the following we shall take

$$\mathcal{E} \equiv B_\rho \equiv \{ \varepsilon \in \mathbf{C} : |\varepsilon| \leq \rho \}$$

for a suitable  $\rho > 0$  and  $v^{(0)}$  given by (34). Recall that the input data of the KAM algorithm are the numbers  $(\tilde{M}^{(0)}, M^{(0)}, V^{(0)}, V_1^{(0)}, E^{(0)})$ . To estimate  $\|\partial_\theta^s v^{(0)}\|_\xi$  for  $s = 0, 1$ , we use

$$\|\partial_\theta^s v^{(0)}\|_\xi \leq 2 \sum_{l=1}^{l_0} \rho^l \sum_{n \neq 0} |n|^s |\tilde{u}_n^{(l)}| \cosh(|n| \xi) \equiv V_s^{(0)}$$

( $V_0^{(0)} \equiv V^{(0)}$ ) and then we estimate  $M^{(0)}$  and  $\tilde{M}^{(0)}$  by, respectively,  $1 + V_1^{(0)}$  and  $(1 - V_1^{(0)})^{-1}$ , provided, of course, that  $V_1^{(0)} < 1$  (otherwise we set  $\tilde{M}^{(0)} \equiv \infty$ ).

It remains to estimate the error term. By definition of  $e^{(0)}$

$$\begin{aligned} e^{(0)} &= \sum_{l=1}^{l_0} \varepsilon^l D^2 \tilde{u}_l + \varepsilon f \left( \theta + \sum_{l=1}^{l_0} \varepsilon^l D^2 \tilde{u}_l \right) \\ &= \sum_{l=1}^{l_0} \varepsilon^l D^2 \tilde{u}_l + \sum_{n \neq 0} f_n \sum_{h=1}^{\infty} \varepsilon^h d_{h-1}^{(n)}(\theta) \end{aligned}$$

where the  $f_n$  are the Fourier coefficients of  $f$  and  $d_h^{(n)}(\theta)$  is defined by  $\exp[in(\theta + v^{(0)})] = \sum_{h \geq 0} d_h^{(n)}(\theta) \varepsilon^h$ . Therefore

$$e^{(0)}(\theta; \varepsilon) = \left[ \sum_{l=1}^{l_0} \varepsilon^l \left( D^2 \tilde{u}_l + \sum_{n \neq 0} f_n d_{l-1}^{(n)}(\theta) \right) \right] + \left[ \varepsilon \sum_{n \neq 0} f_n \sum_{l=l_0}^{\infty} \varepsilon^l d_l^{(n)}(\theta) \right] \\ \equiv F_{l_0} + R_{l_0}$$

Notice that if  $f$  is a trigonometric polynomial, so are the  $d_l^{(n)}$  and the  $\tilde{u}_l$  (even though the size grows when  $l$  increases (see the remark at the end of Section 2.2); see below for the explicit formulas, which are similar to (26)–(32)). Thus, the estimate of  $F_{l_0}$  reduces to a finite computation which will be performed on a computer using the interval arithmetic. The bound of  $R_{l_0}$  is based on the following result:

**Lemma.** Let  $v^{(0)}(\theta; \varepsilon)$  and  $d_l^{(n)}(\theta)$  be as above. Given  $\xi > 0$ , define  $a_l^{(n)}(\xi) \geq 0$  for  $0 \leq l \leq l_0$ , so that

$$a_0^{(n)} = |n| \xi \\ a_l^{(n)} \geq |n| \sup_{|\operatorname{Im}(\theta)| \leq \xi} |\tilde{u}_l(\theta)|_{\xi}, \quad 1 \leq l \leq l_0 \quad (35)$$

and define for  $l \geq 0$ ,  $\delta_l^{(n)}$  so that for every  $\varepsilon$

$$\exp \left( \sum_{l=0}^{l_0} a_l^{(n)} \varepsilon^l \right) = \sum_{l=0}^{\infty} \delta_l^{(n)} \varepsilon^l \quad (36)$$

Then

$$|d_l^{(n)}(\theta)|_{\xi} \equiv \sup_{|\operatorname{Im}(\theta)| \leq \xi} |d_l^{(n)}(\theta)| \leq \delta_l^{(n)} \quad (37)$$

and,  $\forall \rho > 0$ ,

$$\left\| \sum_{l=l_0}^{\infty} d_l^{(n)}(\theta) \varepsilon^l \right\|_{\xi, \rho} \leq \sum_{l=l_0}^{\infty} |d_l^{(n)}(\theta)|_{\xi} \rho^l \\ \leq \sum_{l=l_0}^{\infty} \delta_l^{(n)} \rho^l = \exp \left( \sum_{l=0}^{l_0} a_l^{(n)} \rho^l \right) - \sum_{l=0}^{l_0-1} \delta_l^{(n)} \rho^l \quad (38)$$

*Proof.* With arguments similar to those used to derive (26), one sees that  $d_l^{(n)}(\theta)$  and  $\delta_l^{(n)}$  satisfy the following recursion relations:

$$d_l^{(n)}(\theta) \equiv \begin{cases} e^{in\theta}, & l=0 \\ \frac{in}{l} \sum_{h=1}^{\min(l, l_0)} hu_h(\theta) d_{l-h}^{(n)}, & l \geq 1 \end{cases}$$

$$\delta_l^{(n)} \equiv \begin{cases} e^{n\xi}, & l=0 \\ \frac{1}{l} \sum_{h=1}^{\min(l, l_0)} h a_h^{(n)} \delta_{l-h}^{(n)}, & l \geq 1 \end{cases}$$

Let us prove (37) by induction on  $l$ . For  $l=0$

$$|d_0^{(n)}(\theta)|_\xi \leq e^{|n|\xi}$$

Now, fixing  $l \geq 1$  and assuming for  $0 \leq h \leq l-1$

$$|d_h^{(n)}(\theta)|_\xi \leq \delta_h$$

by (35) and the inductive hypotheses one has

$$\begin{aligned} |d_l^{(n)}(\theta)|_\xi &\leq \frac{1}{l} \sum_{h=1}^{\min(l, l_0)} h |n| |u_h(\theta)|_\xi |d_{l-h}^{(n)}(\theta)|_\xi \\ &\leq \frac{1}{l} \sum_{h=1}^{\min(l, l_0)} h a_h^{(n)} \delta_{l-h}^{(n)} = \delta_l^{(n)} \end{aligned}$$

The estimate (38) follows now from (37) and (36). ■

### 2.5. Results

We collect in this section the results of the application of the methods presented above. The rotation numbers  $\omega_1, \omega_2, \omega_3$  satisfy the diophantine condition (4) with  $\tau = 1$  and  $C$  respectively equal to

$$C_1 \equiv \frac{3 + \sqrt{5}}{2}, \quad C_2 \equiv \frac{5 + \sqrt{5}}{2}, \quad C_3 \equiv 2 + \sqrt{2}$$

(see Appendix A for the proof). Both  $\omega_1$  and  $\omega_2$  are irrational noble numbers, namely their continued fraction expansion is definitely one: denoting by

$$[a_0; a_1, a_2, \dots] \equiv a_0 + \frac{1}{a_1 + \frac{1}{a_2 + \dots}}$$

one has

$$\omega_1 = [0; 1, 1, 1, \dots], \quad \omega_2 = [0; 1, 2, 1, 1, 1, \dots], \quad \omega_3 = [0; 1, 2, 2, 2, \dots]$$

The choice of these rotation numbers is related to the fact that such numbers are *badly* approximated by rational numbers, so that the small divisors appearing in the Lindstedt series (and therefore in  $v^{(0)}$ ) are not "too small." It has also been conjectured by MacKay<sup>(21)</sup> and Percival<sup>(27)</sup> that for a certain class of one-parameter mappings the curves with noble rotation numbers are locally the most robust. In particular, the curve with rotation number equal to the golden ratio  $\omega_1$  is the favorite candidate for survival, since  $\omega_1$  is the irrational number worst approximated by rationals. Numerical experiments supporting this statement were performed by Greene<sup>(13)</sup> for the map (SM). However, the golden mean curve is not always the last one to disappear. A numerical computation of the breakdown threshold based on Greene's method (see Section 3.1) indicates that for the map (SM)' actually  $\mathcal{C}'_e(\omega_2)$  might survive longer than  $\mathcal{C}'_e(\omega_1)$  (see Table II).

Table I provides the results of the application of the KAM algorithm. The computations were done on the VAX 8250 of the University of Rome "Tor Vergata" and the program was run at most in 15 h of CPU time.

For a given rotation number  $\omega$ ,  $\varepsilon_r = \varepsilon_r(\omega)$  is the maximal value for which our KAM algorithm ensures the existence of a solution  $u(\theta; \varepsilon)$  of (8) and hence of the invariant curve  $\mathcal{C}_e(\omega)$ . *Maximal* here means that  $\varepsilon_r(\omega)$  is experimentally chosen to be the maximal  $\rho$  for which our KAM algorithm converges [i.e., the KAM condition (18) is satisfied after  $N$  steps] as  $\xi_0$  and (the first few  $\delta_j$ ) are varied. The integer  $l_0$  denotes the order of the initial approximation

$$v^{(l_0)}(\theta; \varepsilon) \equiv \sum_{l=1}^{l_0} \tilde{u}_l(\theta) \varepsilon^l$$

$N$  denotes the number of steps in the KAM algorithm (see Section 2.1); finally,  $\xi_r$  denotes the *width* of the analyticity domain of  $u(\theta; \varepsilon)$ . Notice that if  $\xi_0$  is one of the inputs of the KAM algorithm, and the algorithm converges at the  $N$ th step,  $\xi_r = (\xi_0/4)(1 + 1/2^N)$ .

**Table I. Rigorous Lower Estimates for the Existence of KAM Curves**

Curve	$l_0$	$\varepsilon_r$	$N$	$\xi_r$
$\mathcal{C}_e(\omega_1)$	190	0.838	6	$5.07 \times 10^{-3}$
$\mathcal{C}_e(\omega_2)$	190	0.77	5	$5.15 \times 10^{-3}$
$\mathcal{C}_e(\omega_3)$	160	0.76	5	$5.15 \times 10^{-3}$
$\mathcal{C}'_e(\omega_1)$	60	0.4	7	$5.03 \times 10^{-3}$
$\mathcal{C}'_e(\omega_2)$	60	0.39	7	$5.03 \times 10^{-3}$



### 3. EXPERIMENTAL METHODS

In this section we briefly discuss some numerical experiments for parameter values near to critical. The discussion is sketchy and aims at pointing out qualitative phenomena without attempting a systematic quantitative analysis, which, we believe, deserves further investigation.

#### 3.1. Greene’s Method

There exist various numerical methods designed to estimate the critical value at which a given KAM torus *disappears*. An excellent one is a method worked out by J. Greene. He conjectures that the breakdown of an invariant curve  $\mathcal{C}_\varepsilon(\omega)$  is related to a sudden change from (linear) stability to instability of the periodic orbits “approaching”  $\mathcal{C}_\varepsilon(\omega)$ . More precisely, he considers a family of periodic orbits with period  $q_j$  and rotation number  $p_j/q_j$  given by the rational approximants to the irrational rotation number  $\omega$  (see Appendix A) and, as  $j$  increases, the trace of the associated Floquet matrices is studied (see ref. 26 for another interesting method for the numerical evaluation of  $\varepsilon_b$ ).

We summarize in Table II the results for the curves considered in Section 2, denoting by  $\varepsilon_G$  the value obtained applying Greene’s method.

#### 3.2. $\varepsilon$ -Expansion Criterion

Following ref. 6, we present a (rather crude) numerical experiment based on the direct construction of the KAM curve.

We saw in Section 2 that a KAM curve can be parametrized by

$$\begin{cases} x = \theta + u(\theta; \varepsilon) \\ y = \omega + u(\theta; \varepsilon) - u(\theta - \omega; \varepsilon), \end{cases} \quad \theta \in \mathbf{T}$$

**Table II. Experimental Evaluation of the Critical Parameter at Which KAM Curves Disappear**

Curve	$\varepsilon_G$
$\mathcal{C}_\varepsilon(\omega_1)$	0.9716
$\mathcal{C}_\varepsilon(\omega_2)$	0.9044–0.9045
$\mathcal{C}_\varepsilon(\omega_3)$	0.908–0.909
$\mathcal{C}'_\varepsilon(\omega_1)$	0.6013–0.6014
$\mathcal{C}'_\varepsilon(\omega_2)$	0.7212–0.7214

**Table III. Experimental Evaluation of the  $\epsilon$ -Radius of Convergence of KAM Curves**

Curve	$\epsilon_n$
$\mathcal{C}_\epsilon(\omega_1)$	0.973
$\mathcal{C}_\epsilon(\omega_2)$	0.905–0.906
$\mathcal{C}_\epsilon(\omega_3)$	0.912–0.913
$\mathcal{C}'_\epsilon(\omega_1)$	0.52
$\mathcal{C}'_\epsilon(\omega_2)$	0.5

and that an explicit polynomial approximation

$$\tilde{u}^{(l_0)}(\theta; \epsilon) \equiv \sum_{l=1}^{l_0} \tilde{u}_l(\theta) \epsilon^l$$

can be constructed. If  $l_0$  is large enough and if  $|\epsilon| < \rho_a$  [see (33)], then for any  $\theta$  the point  $(x_0, y_0) = (\theta + u_{l_0}(\theta; \epsilon), \omega + u_{l_0}(\theta; \epsilon) - u_{l_0}(\theta - \omega; \epsilon))$  lies very close to the true KAM curve. So that if we take  $(x_0, y_0)$  as initial point and if we look at the iterates  $F_\epsilon^n(x_0, y_0)$  we expect to see a regular graph in the  $(x, y)$  plane which should be a good approximation to the KAM curve. When  $\epsilon$  becomes equal to  $\rho_a$ , the series  $\sum u_l(\theta) \epsilon^l$  will no longer converge

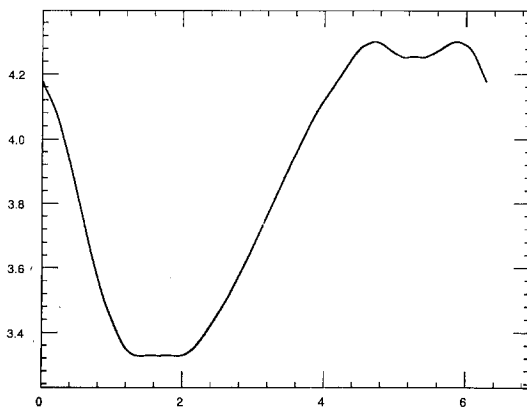


Fig. 1. Standard map,  $\epsilon = 0.97135$ ,  $10^6$  iterations of

$$(x_0, y_0) \equiv \left( 0, \omega_1 + \sum_{l=1}^{200} \tilde{u}_l(\omega, \epsilon) \epsilon^l \right), \quad \omega_1 \equiv (\sqrt{5} - 1) \pi$$

The initial point  $(x_0, y_0)$  is obtained through a 200-truncation of  $\epsilon$ -power series of the parametric representation of the invariant curve (see Section 2 for more details).

(at least for some values of  $\theta$ ) and we expect that the iterates  $F_\varepsilon^n(x_0, y_0)$  will eventually wander in phase space, covering in a “chaotic” way open regions. The number of iterations we monitored (for the models at hand) was of the order of  $10^6$  and observations were made at various scales. Long chains of elliptic islands were considered “regular behavior,” while “chaotic” regime was assigned to orbits which after  $10^4$ – $10^6$  iterations “covered” open regions. Table III shows the application of this method to the maps considered in Section 2:  $\varepsilon_n$  denotes the numerical transition value at which the iterates  $F_\varepsilon^n(x_0, y_0)$  do not seem to lie on a graph.

This technique, besides visualizing the graph of the invariant curve, provides a rough estimate of  $\rho_a$ . In the case of the standard map (*SM*),  $\rho_a \simeq \varepsilon_G$  (compare Tables II and III) which in particular indicates that  $\varepsilon_a \simeq \varepsilon_b$ . A different phenomenon shows up when one compares the results of the two methods in the case of the map (*SM'*): for both  $\omega_1$  and  $\omega_2$  there is a relatively large discrepancy between the  $\varepsilon$ -expansion and Greene methods. A plausible explanation relies on the remark that the  $\varepsilon$ -expansion criterion provides an estimate on the minimal radius of analyticity in the complex  $\varepsilon$ -plane, while Greene’s value relates to the *real* breakdown threshold.

A numerical study of this phenomenon indicates that for the standard map the domain of  $\varepsilon$ -analyticity of  $\sum u_l(\theta) \varepsilon^l$  (for typical values of  $\theta$ ) is a circle with radius equal to Greene’s value,<sup>(3)</sup> while the same experiment for the two-frequency map<sup>(2)</sup> suggests that the domain of analyticity might be at least in “first approximation” an ellipse with the minor semiaxis approximately equal to the value obtained by the  $\varepsilon$ -expansion criterion and the major semiaxis about equal to Greene’s value.

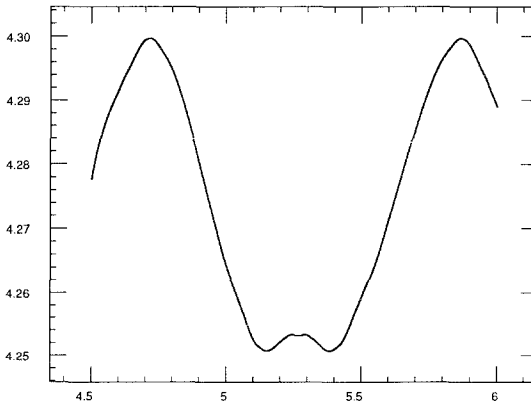


Fig. 2. Magnification of Fig. 1.

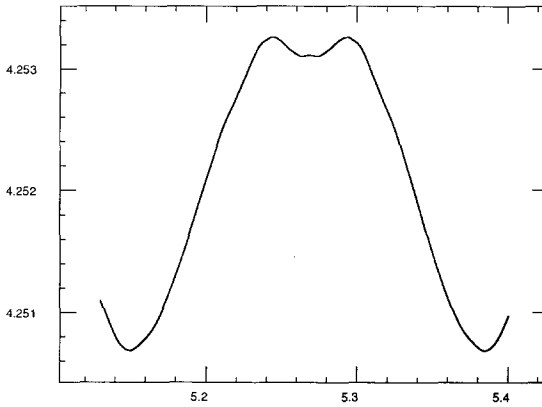


Fig. 3. Magnification of Fig. 1.

### 3.3. Self-Similarity

For the standard map, as already mentioned, it is believed that  $\rho_a = \varepsilon_a = \varepsilon_b$ ; if this is so,  $(x_0, y_0)$  computed as described in the previous section (with  $l_0 = 190$ ) yields a very good approximation of a point on the invariant curve for  $\varepsilon \leq \rho_a$ . By iterating  $10^6$  times such a point for  $\varepsilon = 0.97135$  we obtain Fig. 1. Critical curves have a very special role in the renormalization approach<sup>(10,20)</sup> and one of their main properties should be the “self-similar” structure. Magnifying the interval  $[4.5, 6]$  of the  $x$  axis containing the two maxima of the curve, we obtain the second picture (Fig. 2). Successive magnifications around the local maxima (respectively, minima) suggest that at each step the graph is an upsetting of the previous picture on a different scale (Figs. 3–5). After a few magnifications this

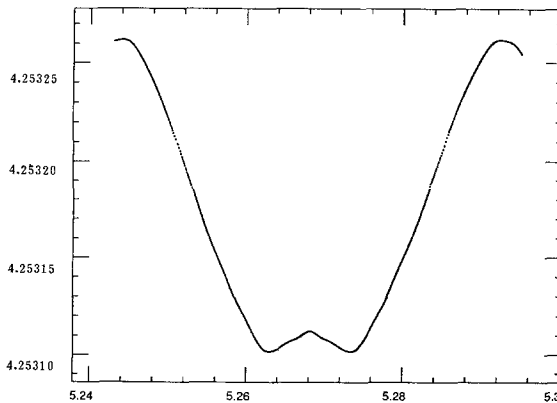


Fig. 4. Magnification of Fig. 1.

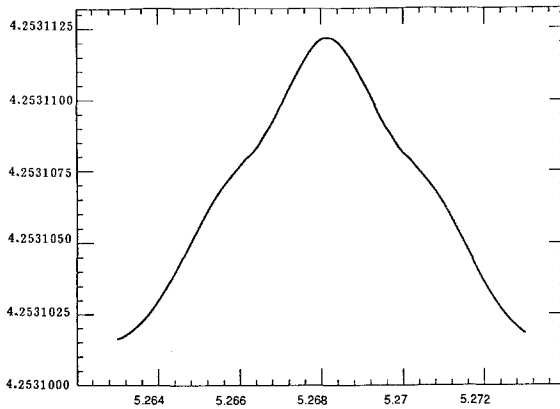


Fig. 5. Magnification of Fig. 1.

phenomenon stops; the number of self-similar rescalings depends on how close is  $\varepsilon$  to the transition value (see ref. 21 and references therein for more on this theme).

### APPENDIX A. COMPUTATION OF THE DIOPHANTINE CONSTANTS

Here we compute the *diophantine constants* for

$$\omega_1 \equiv \frac{\sqrt{5}-1}{2}, \quad \omega_2 \equiv \frac{\sqrt{5}+5}{10}, \quad \omega_3 \equiv \frac{\sqrt{2}}{2}$$

More precisely, we shall prove that (for  $i = 1, 2, 3$ )

$$\left| \omega_i - \frac{p}{q} \right| \geq \frac{1}{C_i q^2}, \quad \forall p, q \in \mathbf{Z}, \quad q \neq 0 \tag{39}$$

with

$$C_1 \equiv \frac{3+\sqrt{5}}{2}, \quad C_2 \equiv \frac{5+\sqrt{5}}{2}, \quad C_3 \equiv 2 + \sqrt{2} \tag{40}$$

Let us recall a few standard facts from the theory of continued fractions.<sup>(16)</sup> Let  $\omega$  be a positive irrational number and denote by  $[a_0; a_1, a_2, \dots]$ ,  $a_k \in \mathbf{N}$  its continued fraction expansion, i.e.,

$$\omega \equiv a_0 + \frac{1}{a_1 + \frac{1}{a_2 + \dots}}$$

Denote also, as usual,

$$\frac{p_k}{q_k} \equiv [a_0; a_1, \dots, a_k], \quad r_k \equiv [a_k; a_{k+1}, \dots]$$

Then, the following standard relations hold<sup>(16)</sup>:

$$p_k = p_{k-1}a_k + p_{k-2}, \quad q_k = q_{k-1}a_k + q_{k-2}$$

for any  $k \geq 1$ , having set  $p_{-1} \equiv 1, q_{-1} \equiv 0, p_0 \equiv a_0, q_0 \equiv 1$ ; also,

$$p_{k-1}q_{k-2} - p_{k-2}q_{k-1} = (-1)^k, \quad \forall k \geq 1; \quad \frac{p_{2k}}{q_{2k}} \nearrow \omega \searrow \frac{p_{2k+1}}{q_{2k+1}} \quad (41)$$

$$\frac{1}{q_k(q_k + q_{k+1})} < \left| \omega - \frac{p_k}{q_k} \right| < \frac{1}{q_k q_{k+1}}; \quad \omega = \frac{r_k p_{k-1} + p_{k-2}}{r_k q_{k-1} + q_{k-2}} \quad (42)$$

**Lemma A1.** Let  $\Phi: [1, \infty) \rightarrow [1, \infty)$  be a continuous nondecreasing function. Then from

$$|\omega q_k - p_k| \geq \frac{1}{\Phi(q_k)}, \quad \forall k \geq 0$$

it follows that

$$|\omega q - p| \geq \frac{1}{\Phi(q)}, \quad \forall q \neq 0$$

*Proof.* If  $p/q = p_k/q_k$  for some  $k$ , there is nothing to prove. Assume therefore that  $p/q \neq p_k/q_k, \forall k \geq 0$ . Then three cases are possible: (i)  $p/q < p_0/q_0 \equiv a_0$ , (ii)  $p/q > p_1/q_1$ , or (iii)  $p/q \in I_k$ , where  $I_k \equiv (p_{k+1}/q_{k+1}, p_{k-1}/q_{k-1})$  for  $k$  odd and  $I_k \equiv (p_{k-1}/q_{k-1}, p_{k+1}/q_{k+1})$  for  $k$  even.

In case (i):

$$|\omega q - p| \geq \left| \omega - \frac{p}{q} \right| > |\omega - a_0| = \left| \omega - \frac{p_0}{q_0} \right| \geq \frac{1}{\Phi(q_0)} = \frac{1}{\Phi(1)} \geq \frac{1}{\Phi(q)}$$

In case (ii):

$$\left| \frac{p}{q} - \omega \right| > \left| \frac{p}{q} - \frac{p_1}{q_1} \right| \geq \frac{1}{qq_1} \Rightarrow |p - \omega q| > \frac{1}{q_1} = \frac{1}{a_1}$$

On the other hand,  $|\omega - a_0| \leq 1/a_1$ ; therefore

$$|\omega q - p| > |\omega - p_0| = |\omega q_0 - p_0| \geq \frac{1}{\Phi(q_0)} \geq \frac{1}{\Phi(q)}$$

In case (iii), by (41),

$$\begin{aligned} \frac{1}{qq_{k-1}} &\leq \left| \frac{p}{q} - \frac{p_{k-1}}{q_{k-1}} \right| \left| \frac{p_{k+1}}{q_{k+1}} - \frac{p_{k-1}}{q_{k-1}} \right| < \left| \frac{p_k}{q_k} - \frac{p_{k-1}}{q_{k-1}} \right| \\ &= \frac{1}{q_k q_{k-1}} \Rightarrow q > q_k \end{aligned}$$

Again by (41),

$$\left| \omega - \frac{p}{q} \right| > \left| \frac{p_{k+1}}{q_{k+1}} - \frac{p}{q} \right| \geq \frac{1}{qq_{k+1}} \Rightarrow |\omega q - p| \geq \frac{1}{q_{k+1}}$$

but, by (42),  $|\omega q_k - p_k| \leq 1/q_{k+1}$  and since  $q > q_k$ , Lemma 1 follows. ■

**Lemma A2.** For all  $k \geq 0$

$$\left| \omega - \frac{p_k}{q_k} \right| = \frac{1}{\sigma_k q_k^2}$$

with  $\sigma_k \equiv r_{k+1} + q_{k-1}/q_k$ .

*Proof.* By (42) and (41)

$$\begin{aligned} \left| \omega - \frac{p_k}{q_k} \right| &\equiv \left| \frac{r_{k+1} p_k + p_{k-1}}{r_{k+1} q_k + q_{k-1}} - \frac{p_k}{q_k} \right| \equiv \frac{1}{q_k (r_{k+1} q_k + q_{k-1})} \\ &= \frac{1}{q_k^2} \frac{1}{(r_{k+1} + q_{k-1}/q_k)} \equiv \frac{1}{q_k^2 \sigma_k} \quad \blacksquare \end{aligned}$$

By Lemma 1 it is enough to check (39) for  $(p, q) = (p_k, q_k)$  and by Lemma 2 we can take  $C = \sup_{k \geq 0} \sigma_k$ . Since, as one easily checks,

$$\omega_1 = [0; 1, 1, 1, \dots] \equiv [0; 1^\infty], \quad \omega_2 = [0; 1, 2, 1^\infty], \quad \omega_3 = [0; 1, 2^\infty]$$

one finds (the superscripts refers to the index of the  $\omega$ 's)

$$\begin{aligned} r_{k+1}^{(1)} &= \frac{\sqrt{5} + 1}{2} \quad (\forall k \geq 0) \\ r_1^{(2)} &= \frac{5 - \sqrt{5}}{2}, \quad r_2^{(2)} = \frac{\sqrt{5} + 3}{2}; \quad r_k^{(2)} = \frac{\sqrt{5} + 1}{2} \quad (\forall k \geq 3) \\ r_1^{(3)} &= \sqrt{2}, \quad r_k^{(3)} = 1 + \sqrt{2} \quad (\forall k \geq 2) \end{aligned}$$

From

$$\frac{q_{-1}^{(i)}}{q_0^{(i)}} = 0, \quad \frac{q_0^{(i)}}{q_1^{(i)}} = 1, \quad \frac{q_k^{(i)}}{q_{k+1}^{(i)}} < 1 \quad (i = 1, 2, 3, \quad \forall k \geq 1)$$

(39) and (40) follow. Notice that one might get better estimates for  $k \geq k_0 > 0$  using the general identity

$$\frac{q_k}{q_{k-1}} = [a_k; a_{k-1}, \dots, a_1], \quad \forall k \geq 1$$

### APPENDIX B

In this section we show how to obtain an upper bound on the quantity

$$\sigma_l(\delta) = \left[ \sum_{n=1}^{\infty} \left( \frac{n^l}{\sin(n\omega/2)} \right)^2 e^{-\delta n} \right]^{1/2}, \quad l = 0, 1 \tag{43}$$

where  $\omega \in (0, 2\pi)$  satisfies (4) with  $\tau = 1$ . The idea is to split the sum into a finite part, which can be “explicitly” evaluated, plus a remainder for which analytical estimates can be proved.

**Lemma B1.** Let  $\sigma_l(\delta)$  be as in (43); then for  $l = 0, 1$ ,  $\sigma_l(\delta)$  can be estimated by

$$s_l(\delta) \equiv \left[ \sum_{n=1}^{N-1} \left( \frac{n^l}{\sin(n\omega/2)} \right)^2 e^{-\delta n} + S_l^{(N)} \right]^{1/2}, \quad N \in \mathbb{N}$$

where, denoting  $\alpha \equiv \delta(1 + \omega)$ ,

$$\begin{aligned} S_0^{(N)} &\equiv \frac{\pi^2 C^2}{4} (1 - e^{-\delta}) e^{\delta/2} e^{-\alpha(N-1)} \frac{1}{\alpha^3} [2 + (2N + 1)\alpha + N^2\alpha^2] \\ S_1^{(N)} &\equiv \frac{\pi^2 C^2}{4} (1 - e^{-\delta}) e^{\delta/2} e^{-\alpha(N-1)} \frac{1}{\alpha^5} [24 + (24N + 36)\alpha \\ &\quad + (12N^2 + 24N + 14)\alpha^2 + (4N^3 + 6N^2 + 4N + 1)\alpha^3 + N^4\alpha^4] \end{aligned} \tag{44}$$

*Proof.* Let

$$b_n \equiv \sum_{N \leq k \leq n} \frac{1}{\sin^2(k\omega/2)} \quad \text{for } n \geq N \quad \text{and} \quad b_{N-1} = 0$$



Then, since  $b_n - b_{n-1} = 1/\sin^2(n\omega/2)$ , it follows that

$$\begin{aligned} \sum_{n=N}^{\infty} \left( \frac{n^l}{\sin(n\omega/2)} \right)^2 e^{-\delta n} &= \sum_{n=N}^{\infty} n^{2l} e^{-\delta n} (b_n - b_{n-1}) \\ &= \sum_{n=N}^{\infty} n^{2l} e^{-\delta n} b_n - \sum_{n=N}^{\infty} (n+1)^{2l} e^{-\delta n} e^{-\delta} b_n \\ &\leq (1 - e^{-\delta}) \sum_{n=N}^{\infty} n^{2l} e^{-\delta n} b_n \\ &\leq (1 - e^{-\delta}) \frac{\pi^2 C^2}{12} \sum_{n=N}^{\infty} n^{2l+2} e^{-\delta n} \end{aligned}$$

where in the last inequality we used Rüssmann’s estimate<sup>(28)</sup>

$$\begin{aligned} |b_n| &= \sum_{N \leq k \leq n} \frac{1}{\sin^2(k\omega/2)} \leq \sum_{1 \leq k \leq n} \frac{1}{4 \min_{l \in \mathbb{Z}} |(\omega/2\pi)k - l|} \\ &\leq \frac{\pi^2 C^2}{12} n^2 \end{aligned}$$

Now using that for any  $k \geq 0$

$$\sum_{n=N}^{\infty} n^k e^{-\delta n} = (-1)^k \frac{d^k}{d\delta^k} \frac{e^{-\delta N}}{1 - e^{-\delta}}$$

and the estimate

$$\frac{e^{-\delta}}{1 - e^{-\delta}} < \frac{1}{\delta}, \quad \forall \delta > 0$$

one has

$$\sum_{n=N}^{\infty} \left( \frac{n^l}{\sin(n\omega/2)} \right)^2 e^{-\delta n} < S_l^{(N)}$$

with  $S_l^{(N)}$  as in (44). ■

### APPENDIX C

Let us denote by  $\mathcal{R}$  a certain set of representable numbers on a given computer (for example,  $\mathcal{R}$  may be the set of “REAL \* 8” numbers represented in G-floating on a VAX 8250<sup>(29)</sup>). The result of an elementary

operation (i.e., addition, subtraction, multiplication, or division) between two numbers in  $\mathcal{R}$  may not be in  $\mathcal{R}$  and, therefore, the result given by the computer is in such a case approximated. However, it is usually possible (as in the case of the VAX) to give *lower* and *upper* bounds in terms of representable numbers of the actual result. In other words, it is possible to trap the result of an elementary operation between  $x, y \in \mathcal{R}$  in an *interval* with endpoints still in  $\mathcal{R}$  (the size of such an interval will be about equal to the *precision* one is working with).

*Interval arithmetic* consists in substituting real numbers with (possibly closed) intervals with endpoints in  $\mathcal{R}$  and in substituting elementary algebra on real numbers with (straightforward) algebra on intervals. Let us try to make this clear with an example. Imagine we want to compute with interval arithmetic the number  $-1/\pi^2$ . Let  $1 \in [1_-, 1_+]$ ,  $\pi \in [\pi_-, \pi_+]$  with  $1_{\pm}, \pi_{\pm} \in \mathcal{R}$ . Notice that necessarily  $\pi_- < \pi < \pi_+$ , but that it is (usually) true that  $1 \in \mathcal{R}$ , so that one will take  $1_- = 1_+ = 1$ . Now, if  $x, y \in \mathcal{R}$  and  $\langle \cdot, \cdot \rangle$  denotes one of the elementary operations, we denote by  $\langle x, y \rangle_+, \langle x, y \rangle_-$  the best, respectively, upper and lower bounds in  $\mathcal{R}$  on the number  $\langle x, y \rangle$ :  $\langle x, y \rangle_{\pm} \in \mathcal{R}$  and  $\langle x, y \rangle_+ = \min\{r \in \mathcal{R}: r \geq \langle x, y \rangle\}$ ,  $\langle x, y \rangle_- = \max\{r \in \mathcal{R}: r \leq \langle x, y \rangle\}$ . Then  $\pi^2 \in [(\pi_- * \pi_-)_-, (\pi_+ * \pi_+)_+] \equiv [a_-, a_+]$ ,  $1/\pi^2 \in [(1_-/a_+)_-, (1_+/a_-)_+] \equiv [b_-, b_+]$ , and finally, since the change of sign is (usually) an *exact* operation among representable numbers (i.e., if  $r \in \mathcal{R}$ , then  $-r \in \mathcal{R}$ ),  $1/\pi^2 \in [-b_+, -b_-]$ .

An automatization of this type of procedure allows one to keep track of errors in long computations.

## REFERENCES

1. V. I. Arnold, Proof of a theorem by A. N. Kolmogorov on the invariance of quasiperiodic motions under small perturbations of the Hamiltonian, *Russ. Math. Surv.* **18**:9 (1963).
2. A. Berretti, A. Celletti, L. Chierchia, and C. Falcolini, work in progress.
3. A. Berretti and L. Chierchia, On the complex analytic structure of the golden invariant curve for the standard map, *Nonlinearity* **3**:39 (1990).
4. J.-B. Bost, Tores invariants des systèmes dynamiques Hamiltoniens, *Sem. Bourbaki* **639**:113 (1984–1985).
5. A. Celletti and L. Chierchia, Rigorous estimates for a computer-assisted KAM theory, *J. Math. Phys.* **28**:2078 (1987).
6. A. Celletti and L. Chierchia, Construction of analytic KAM surfaces and effective stability bounds, *Commun. Math. Phys.* **118**:119 (1988).
7. A. Celletti and L. Chierchia, A computer-assisted approach to small-divisors problems arising in Hamiltonian mechanics, in *Computer-Aided Proofs in Analysis*, K. R. Meyer and D. S. Schmidt, eds. (Springer-Verlag, 1991).
8. R. De La Llave and D. Rana, Accurate strategies for K.A.M. bounds and their implementation, in *Computer-Aided Proofs in Analysis*, K. R. Meyer and D. S. Schmidt, eds. (Springer-Verlag, 1991).

9. J.-P. Eckmann and P. Wittwer, Computer methods and Borel summability applied to Feigenbaum's equation, in *Springer Lecture Notes in Physics*, No. 227 (Springer-Verlag, 1985).
10. D. F. Escande and F. Doveil, Renormalization method for computing the threshold of the large-scale stochastic instability in two degrees of freedom Hamiltonian systems, *J. Stat. Phys.* **26**:257 (1981).
11. G. Gallavotti, *The Elements of Mechanics* (Springer-Verlag, New York, 1983).
12. D. Goroff, unpublished (1983).
13. J. M. Greene, A method for determining a stochastic transition, *J. Math. Phys.* **20**:1183 (1979).
14. M. Herman, Sur la conjugaison différentiable des difféomorphismes du cercle a des rotations, in *IHES Publications Mathématiques*, No. 49 (1979).
15. M. Herman, Sur les courbes invariantes pour les difféomorphismes de l'anneau, *Astérisque* **I**:103–104 (1983).
16. A. Khintchine, *Continued Fractions* (Noordhoff, Groningen, 1963).
17. D. E. Knuth, *The Art of Computer Programming*, Vol. 2 (Addison-Wesley, 1968).
18. A. N. Kolmogorov, On the conservation of conditionally periodic motions under small perturbation of the Hamiltonian, *Doklady Akad. Nauk SSR* **98**:469 (1954).
19. O. E. Lanford III, Computer assisted proofs in analysis, *Physics A* **124**:465 (1984).
20. R. S. MacKay, A renormalization approach to invariant circles in area-preserving maps, *Physica* **7D**:283 (1983).
21. R. S. MacKay, Transition to chaos for area-preserving maps, in *Lectures Notes in Physics*, No. 247 (Springer-Verlag, 1985), p. 390.
22. R. S. MacKay and I. C. Percival, Converse KAM: Theory and practice, *Commun. Math. Phys.* **98**:469 (1985).
23. J. N. Mather, Existence of quasiperiodic orbits for twist homeomorphisms of the annulus, *Topology* **21**:457 (1982).
24. J. N. Mather, Nonexistence of invariant circles, *Erg. Theory Dynam. Syst.* **4**:301 (1984).
25. J. Moser, On invariant curves of area-preserving mappings of an annulus, *Nach. Akad. Wiss. Göttingen Math. Phys. Kl. II* **1**:1 (1962).
26. A. Olvera and C. Simó, An obstruction method for the destruction of invariant curves, *Physica* **26D**:181 (1987).
27. I. C. Percival, Chaotic boundary of a Hamiltonian map, *Physica* **6D**:67 (1982).
28. H. Rüssmann, On optimal estimates for the solutions of linear difference equations on the circle, *Celestial Mechanics* **14**:33 (1976).
29. *Vax Architecture Handbook*, Digital Equipment Corporation (1981).